Earthq Eng & Eng Vib (2021) 20: 89-100 **DOI**: https://doi.org/10.1007/s11803-021-2007-x

Introducing an effective coherence function to generate non-uniform ground motion on topographic site using time-domain boundary element method

Mohsen Isari† and Reza Tarinejad‡

Faculty of Civil Engineering, University of Tabriz, Tabriz, East Azerbaijan Province, Iran

Abstract: In this study, a comprehensive parametric analysis was performed on non-uniform excitation of V-shaped topography using the boundary element method in time domain. For this purpose, wave scattering analysis was carried out on a topography subjected to the SV-wave for different predominant frequencies and shape ratios. Based on the numerical results, new coherence and time delay functions are proposed to generate non-uniform ground motion for topographic irregularities. The efficiency and accuracy of the proposed functions for real engineering problems are indicated by comparison with observations reported in previous literature.

Keywords: site effect; time delay; boundary element method; amplification; coherence function

1 Introduction

Studies have shown that topographic irregularities such as canyons and hills influence the seismic behavior of structures. As a result, a complex pattern of displacement is generated in the canyon wall that is different from one point to another point on this surface in terms of amplitude and phase. In seismic analysis of structures, which have great surface contact with the foundation, considering non-uniform excitation of support is of great importance. Numerical investigation of the effects of topographic features on the ground response and ground motion at different points of support is one of the ways of achieving non-uniform excitation (Gatmiri *et al*., 2008; Sohrabi-Bidar and Kamalian, 2013; Hesami *et al*., 2015; Tarinejad *et al*., 2019, 2020). Among numerical methods, boundary element method has a wide application for solving wave propagation problems. This method is suitable for infinite domains since discretization is performed on the boundary of the domain, and therefore the number of degrees of freedom is greatly reduced. In this regard, Mossessian and Dravinski (1990a) investigated the amplification effect through studying a three-dimensional canyon. They used the indirect boundary integral formulation to solve the problem. The results of the two-and three-dimensional models show that the accuracy of models greatly depends on the angle, type, and frequency of the incident waves. Zhang and Chopra (1991) obtained the formulation of the direct boundary element method for investigating the scattering of seismic waves on a canyon with an infinite length in homogeneous viscoelastic half-space. Huang and Chiu (1995) examined the topographic amplification phenomenon by installing six seismometers in a canyon in Taiwan. In their study, using the integral method equation in a two-dimensional model and seismograph in the base of the canyon as input, it was shown that recorded and simulated responses have a good agreement. Paolucci (2002) studied displacement amplification induced by irregular steep topography. In this study, first, the natural frequencies of the topography were estimated through Rayleigh′s method and then, based on the spectral element method, the three-dimensional dynamic responses of some real topographies were examined. Zhao and Valliappan (1993) studied canyon topography effects considering incident SH waves by using a combined finite-infinite element method.

Gatmiri *et al*. (2008) investigated spectral acceleration on alluvial and empty canyons with different forms. Kamalian *et al*. (2007) presented numerous studies on half-sine canyons under the effects of P and S wave propagation in vertical direction in two-dimensional mode using the direct boundary elements method. They also developed HYBRID software code to analyze different types of topographic constructions, including canyons and hills. Kamalian *et al*. (2003, 2006) found that to achieve the required accuracy in analyses, the time step in hybrid methods should be at least equal to half of the time step used in the method of boundary elements. Sohrabi-Bidar *et al*.

Correspondence to: Reza Tarinejad, Faculty of Civil Engineering, University of Tabriz, 29 Bahman Blvd, 51666, Tabriz, Iran
Tel: +98 413 3392386
E-mail: r_tarinejad@tabrizu.ac.ir
†Assistant Professor; ‡Associate Professor
Received November 13, 2018; **Accepted** November 11, 2019

(2010) provide a three- dimensional boundary element formulation method in time domain for the analysis of seismic waves from the topographic construction. In order to demonstrate the accuracy of the presented analysis, they formulated several types of analysis on different constructions considering canyons and hills.

Sohrabi-Bidar *et al*. (2013) used three-dimensional direct boundary elements for parametric study of the response of V-shape canyons. Tarinejad *et al*. (2013, 2019) studied the effects of topographic amplification using a three-dimensional boundary element method in the frequency domain. They examined the effects of different parameters on the amplification by earthquake, such as frequency, angle of the incident wave, the characteristics of the material and the shape of the canyon. Various models of coherence function have been developed by several researchers, including Luco and Wong (1986), Abrahamson (1993), and Harichandarn and Vanmarcke (1986).

Der Kiureghian *et al*. (1992) examined the development of a spectral analysis method for non-uniform analysis. The time delay between the records of different points on the topographic surface is also an important factor in generation of non-uniform excitation. Alves *et al*. (2005) examined the issue from another perspective to examine non-uniform excitation. They examined several factors, including time delay on the seismic records in the dam site. Tsaur *et al*. (2008) and Gao (2019) proposed analytical methods to investigate the effect of the geometry of symmetric V-shaped canyons on scattering of incident waves.

In the present study, using the boundary element method in time domain, the seismic response of V-shaped canyons was examined. Therefore, a series of numerical models of V-shaped canyon subjected to the incident vertical Ricker waves was used. By considering different parts of the canyon, the pattern of amplification, the coherence function between the various points in different models, and the time delay relative to the base point were obtained. Finally, effective coherence and time delay functions are proposed to generate non-uniform ground motion on topographic irregularities.

2 Numerical formulation

In this study, numerical modeling was executed using the time-domain boundary element method. The governing equation for an isotropic, elastic, and homogeneous body can be defined by:

$$\left(c_1^2 - c_2^2\right) \times \boldsymbol{u}_{j,ij}(x,t) + c_2^2 \times \boldsymbol{u}_{i,jj}(x,t) + \boldsymbol{b}_i(x,t) - \ddot{\boldsymbol{u}}(x,t) = 0 \quad (1)$$

$\boldsymbol{u}_i$ is the displacement vector; $\boldsymbol{b}_i$ is the body force vector and; c_1 and c_2 are the velocities of the compressional and shear waves, respectively, in which $c_1^2 = (\lambda + 2\mu)/\rho$; $c_2^2 = \mu/\rho$, where λ and μ are the Lame constants, and ρ is the mass density. The corresponding governing boundary integral equation is obtained using the weighted residual method and:

$$c_{ij}(\xi) \times \boldsymbol{u}_j(\xi,t) = \int_{\Gamma} G_{ij} \cdot t_i(x,t)\mathrm{d}\Gamma - \int_{\Gamma} F_{ij} \cdot \boldsymbol{u}_i(x,t)\mathrm{d}\Gamma + \boldsymbol{u}_i^{\mathrm{inc}}(\xi,t) \quad (2)$$

where G_{ij} and F_{ij} are the transient displacement and traction fundamental solutions of Eq. (1), respectively, and exhibits the jth components of the displacements and tractions at point x at time t due to a unit point force applied in direction i at point ξ at preceding time τ. $G_{ij} \cdot t_i$ and $F_{ij} \cdot \boldsymbol{u}_i$ are the Riemann convolution integrals, and c_{ij} is the discontinuity term resulting from the singularity of the traction fundamental solution. In the boundary integral approach to solving the problem by numerical methods, the equation must be expressed as a set of linear equations. The governing integral equation, discretized in the time and spatial domains and the assembled system of equations by writing the equation of each boundary nodes, takes the following matrix form:

$$F^1 \cdot \boldsymbol{U}^N = G^1 \cdot \boldsymbol{T}^N + \boldsymbol{Z}^N \quad (3)$$

in which $\boldsymbol{U}^N$ is the nodal displacement vector, $\boldsymbol{T}^N$ is the traction vector. N is the current time node number, and n denotes the past time node numbers. $\boldsymbol{Z}^N$ includes the effects of the past dynamic history and will be defined as:

$$\boldsymbol{Z}^{\mathrm{N}} = \sum_{n=1}^{N-1} \left(G^{N+1-n} \cdot \boldsymbol{T}^n - \boldsymbol{F}^{N+1-n} \cdot \boldsymbol{U}^n \right) + \boldsymbol{U}^{inc.N} \quad (4)$$

The above proposed formulation was implemented in a general-purpose, nonlinear software code named HYBRID (Kamalian *et al*., 2006). To indicate the accuracy and efficiency of HYBRID, several examples, including site effect analysis of half-space, irregularity topography subjected to incident waves, were solved. This model has been subjected to vertical propagation of the Ricker wave:

$$f(t) = A_{\max} \times [1 - 2 \times (\pi \times f_{\mathrm{p}} \times (t - t_0))^2] \times \mathrm{e}^{-(\pi \times f_{\mathrm{p}} \times (t - t_0))^2} \quad (5)$$

where f_{p}, t_0, and $A_{\max}$ denote the predominant frequency, time shift parameter, and maximum amplitude of the time history respectively. As seen in Fig. 1, the 2D model of V-shaped topography was prepared in different shape ratio (*SR=h/b*). This model was generated with a length of up to 2500 meters from centerline and comprises 430 three-node quadrilateral elements.

3 Results of numerical analysis

Due to the importance of incident shear waves in comparison with compressional waves in engineering analysis, this kind of wave was considered in this

analysis. Wave propagation and amplification behavior are studied in two dimensions. Figure 2 illustrates time-domain dynamic behavior along the 2D V-shaped site subjected to the incident SV wave in the *x*-direction (displacement in the horizontal direction). The results on the canyon are compared for predominant frequencies of 4 and 10 Hz and different shape ratio 0.5 and 1.5, respectively. In this study, incident shear wave velocity of 1100 m/s, Poisson's ratio of 0.33, and density of 2.3 ton/m^3 were used. As can be seen in the time-domain response curves, refraction of the seismic wave begins once the incident shear wave arrives at the base of canyon. After the arrival incident seismic wave, at each of the points on the canyon surface, scattering of waves and propagation of different wave phases around that location was observed. By increasing the distance from the canyon, refraction waves at various points on the canyon surface in each phase interact and cause collection of subsequent P, SV and Rayleigh waves. By increasing the predominant frequency and shape ratio, the wave scattering at corner points of the canyon increases. For farther locations from the canyon, after the refraction of incident waves, the displacement amplitude goes near to zero. Although the arrival time of incident seismic waves for different points of the canyon and half-space is dependent on the canyon geometry and incident wave velocity, in the outside and near the corner of canyon, the interference of scattered incident and refraction waves caused disturbance in the arrival time of seismic waves.

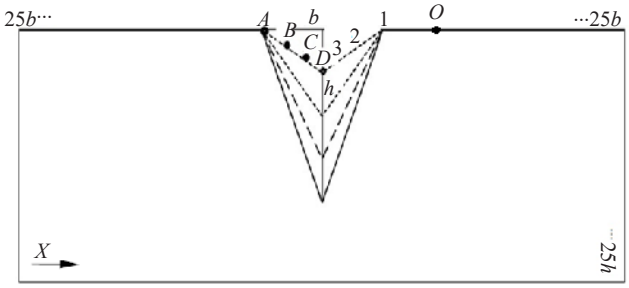

Fig. 1 2D model of the V-shape canyon and considered points

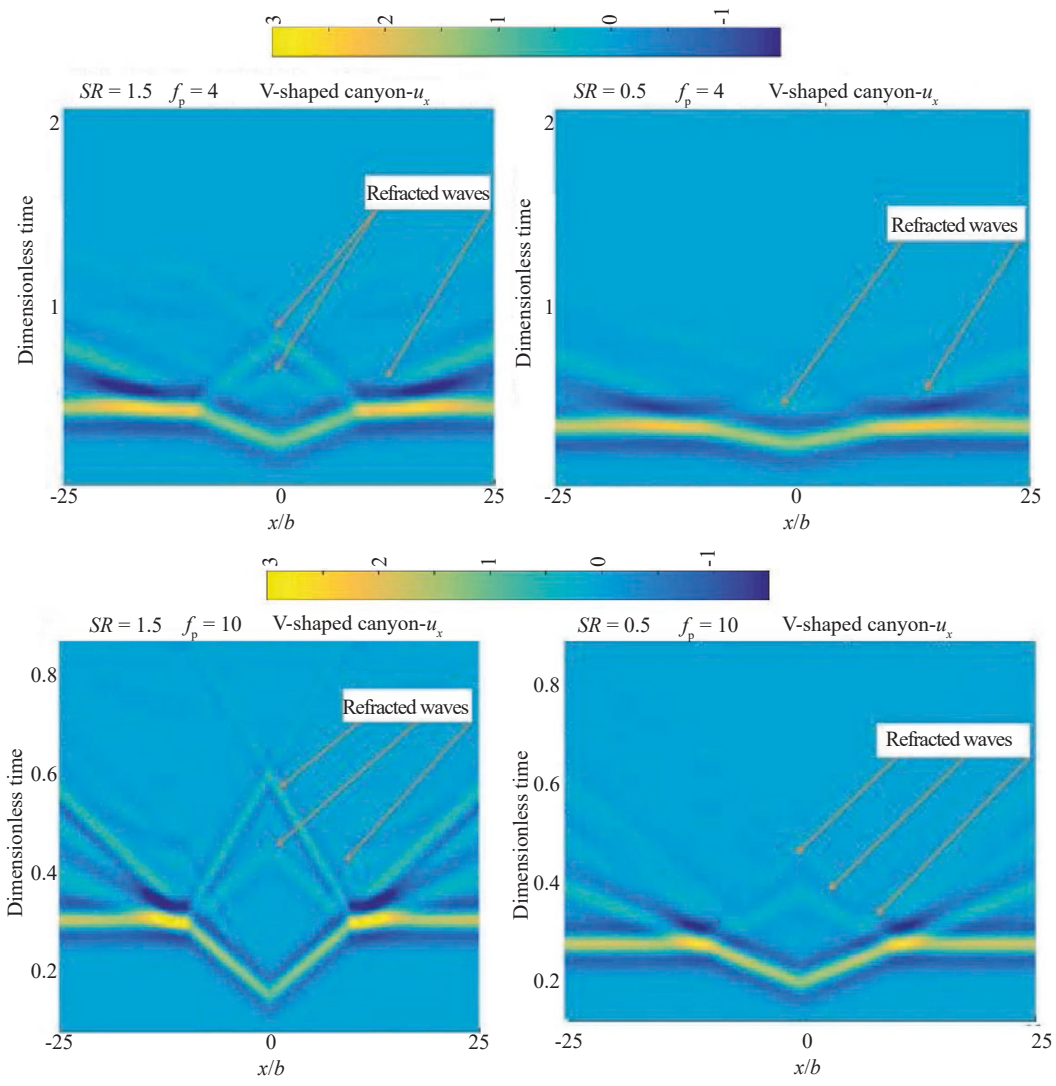

Fig. 2 Time-domain response along the V shape canyon subjected to the incident SV wave in the *X*-direction for predominant frequencies of 4, 10 Hz and *SR* = 0.5, 1.5

3.1 V-shape canyon topographic amplification

This section presents the time domain amplification responses of V-shape topography by seismic wave scattering analysis through the boundary element method. The site responses are evaluated in terms of seismic amplification due to the topographic effect of a V-shape canyon. The influences of parameters such as predominant frequency of the incident wave, point location and shape ratio in *x*-direction are studied. For this purpose, 4 points (see Fig. 1) along the canyon in various elevations were selected. Figures 3 and 4 illustrate time-domain amplification response at the considered points along the site subjected to the incident SV waves polarized in the *x*-direction. The spectral amplification for the V-shape site in the case of the incident SV wave with the predominant frequencies of 1 and 10 and geometry with shape ratios of 0.5, 1, 1.5 and 2 is shown in Figs. 3 and 4, respectively. To obtain the amplification factors of different points relative to the base point, the Fourier amplitude of the motion at various points was divided by the Fourier amplitude of the motion at base points (*D*). The results indicate that amplification factors of different points are not significantly dependent on the location but mainly depend on the predominant frequency of the incident seismic wave.

By increasing the predominant frequency, the range of influences of the frequency on the seismic wave scattering increases. For the constant shape ratio, increasing the frequency leads to the similar pattern of amplification. Except in some cases for very low frequencies, amplification for different points of the canyon in respect to the base point (*D*) was obtained. The amplification curves of the V-shaped topographic feature indicate that increasing the shape ratio of the canyon increases the effect of topography on the ground motion. The same amplification patterns were obtained for the same shape ratios, and different patterns were obtained for different shape ratios.

Increasing both the shape ratios and the predominant frequencies cause very sharp increase in the amplification amplitude, and these two parameters have great influence on the seismic behavior of topographic features. Another parameter that influences amplification is the relative height of the considered points on the canyon. Increasing the elevation of a point increases the amplification factor but does not change the pattern of amplification.

3.2 V-Shape Canyon Time domain displacement response

Figures 5 and 6 illustrates time-domain response at the considered points along the site subjected to the incident SV waves in the x-direction. The results are compared at four points on the canyon for different predominant frequencies 1 and 10 Hz and different shape ratios 0.5, 1, 1.5 and 2, respectively. The same material properties, shear wave velocity of 1100 m/s, Poisson′s ratio of

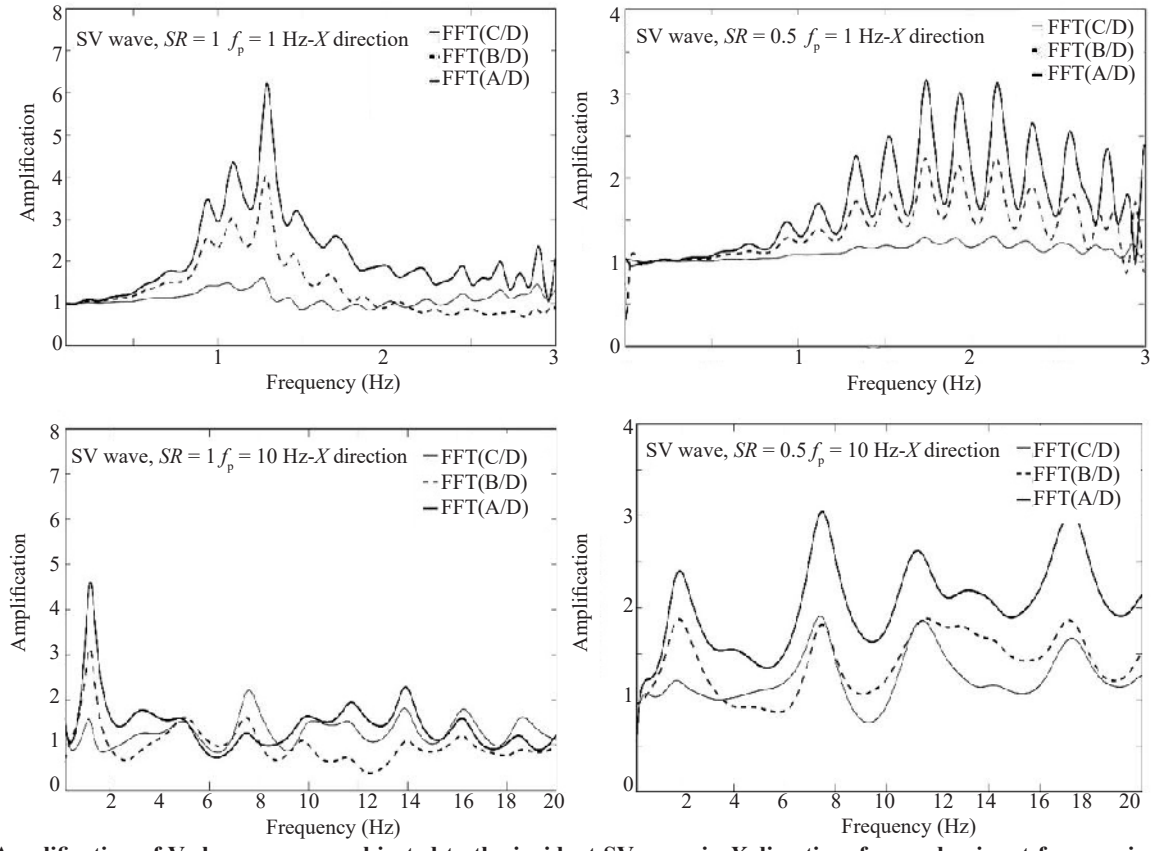

Fig. 3 Amplification of V shape canyon subjected to the incident SV wave in *X*-direction, for predominant frequencies of 1and 10 Hz and *SR* = 0.5, 1

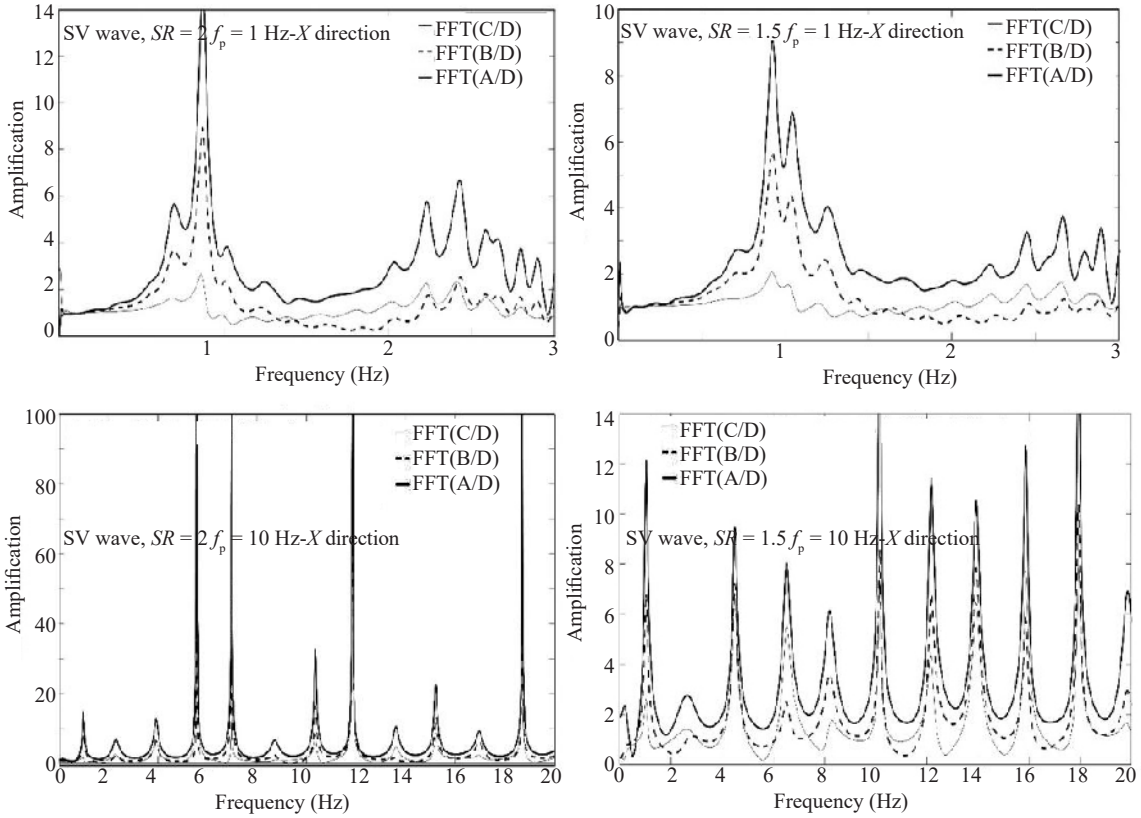

Fig. 4 Amplification of V shape canyon subjected to the incident SV wave in *X*-direction, for predominant frequencies of 1 and 10 Hz and *SR* = 1.5, 2

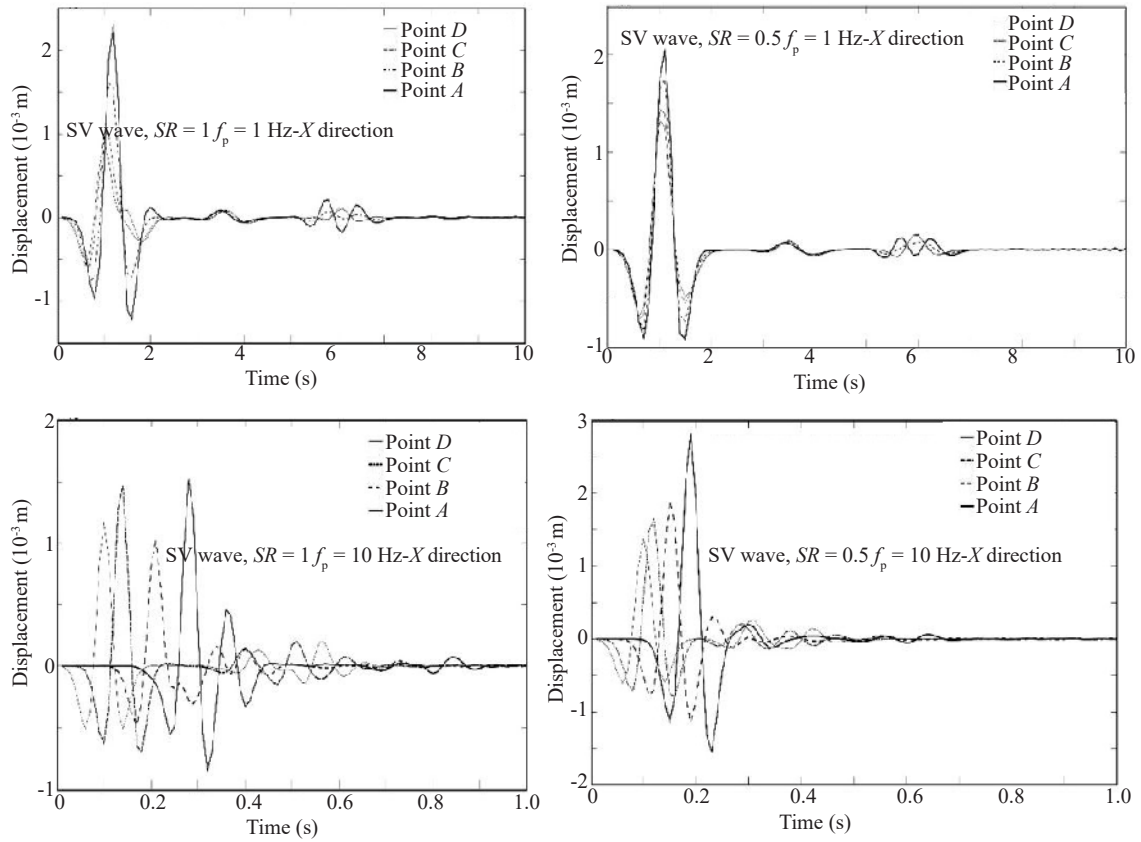

Fig. 5 Time-domain response at the observation points along the V shape canyon subjected to the SV wave in the *X*-direction for predominant frequencies of 1 and 10 Hz and SR = 0.5, 1

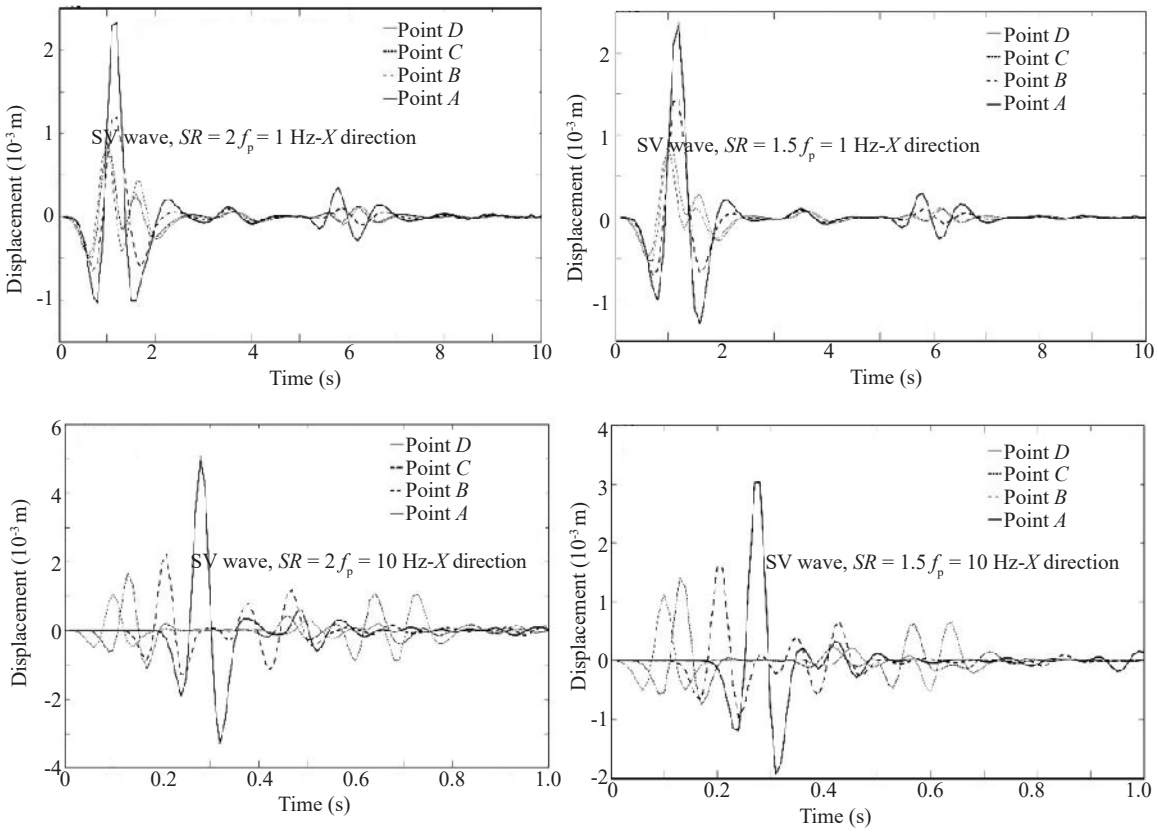

Fig. 6 Time-domain response at the observation points along V shape canyon subjected to the SV wave in the *X*-direction for predominant frequencies of 1and 10 Hz and SR = 1.5, 2

0.33 and density of 2.3 ton/m^3, are used for all analysis. As indicated, the amplitude of displacement evidently depends on the elevation support point at the canyon (see Fig.1). The displacement amplitude gradually increases while the height of considered points is increased. Time delay between the arrival of waves was not observed for the predominant frequency of one. By increasing the predominant frequency, the time delays in arrival of waves were observed. The corner point (*A*) of the canyon in all cases experienced the maximum amplitude. For the shape ratios from 0.5 to 1, amplitude of displacement decreased, but by increasing the shape ratios from 1.5 and 2, the displacement amplitude showed larger values. Maximum displacement amplitude was obtained for the shape ratio of two. By increasing the predominant frequencies, the amplitude of displacement at surface points was increased.

3.3 V-Shape canyon coherence spectrum

The coherence spectrum is used to determine the accuracy of the results of cross-power spectrum between two signals. For example, during an ambient vibration test, the structure is prone to excite from different sources at different distance that causes the values of coherence spectrum for two completely dependent signals to be less than one. So far, some of coherence models have been presented by several researchers mentioned in section 1. The value of this spectrum between two signals is a real number in the range of zero to one. One of the main parameters in coherence behavior with respect to frequency is that the coherence function has resonance at fundamental frequency of structure, and thus in curves pertaining to the amplitude of coherence with respect to frequency, oscillation can be seen. The value of this function represents the quality of the data. It can be claimed that the peaks of the coherence function that are matched to the peaks of the power spectral density and the cross-power spectrum are confidently consistent with the peaks of curve at resonant frequency. In this study, the coherence function for different predominant frequencies and shape ratios was investigated. To obtain this spectrum, Eq. (6) was used:

$$\gamma_{xy}^2 = \frac{\left|S_{xy}(f)\right|^2}{S_{xx}(f)S_{yy}(f)} \tag{6}$$

where γ is the coherence funtion, S_{xy} is cross-power spectral density, S_{xx} is power spectral density. The value of this function in an ideal case at all frequencies will be one. If two signals are not correlated, this value will be zero. Figures 7 and 8 illustrate the coherence function curve at the considered points (between couple points of *O*1, *O*2, *O*3) along the canyon subjected to incident SV

waves in the *X*-direction. The results are compared for different predominant frequencies of 1 and 10 Hz and different shape ratios of 0.5, 1, 1.5 and 2, respectively. For shape ratio of 0.5 and predominant frequency of 1 Hz, the coherence function has maximum value between two points of (*O*3) and the reference point located at the base of the canyon, respectively. Two points (*O*1) and (*O*2) have the same pattern and same value of coherence function relative to the base point. By increasing the predominant frequency, the range of effective frequency increases and at the same shape ratio, coherence function of point (*O*3) have the maximum value. As shown, by increasing the predominant frequency for points on the canyon edge and surface, the coherence spectrum decreases due to the geometry condition. In higher shape ratios and predominant frequencies, the coherence of points decreases such that in SR=2 and f_p=10 Hz, the coherence between all points was near to zero.

The use of the coherence spectrum model is one of the common methods to determine the non-uniform excitation characteristics. These functions are often used in random excitation analysis and are obtained based on dense array recordings on flat surfaces. In order to extend these functions for irregular topographies, comprehensive numerical analyses for different shape ratios from flat surfaces (SR=0) to deep V shape canyons (SR=4) are implemented. The following coherence function was developed by applying multiple regressions to the obtained results based on the effective parameters:

$$Coh_{n,m} = \exp((\omega - f_p{}^2 - \omega \times SR \times f_p - 0.000845 \times \omega \times h_{n,m}^2 - 0.09178 \times h_{n,m} \times f_p{}^2) / c) \quad (7)$$

$Coh_{n,m}$ is the coherence function between two signals (point n) and (point m), $h_{n,m}$ is the height from the base of the canyon, C is the shear wave velocity, SR is the shape ratio and f_p is the predominant frequency. To investigate the efficiency and accuracy of the proposed function, a comparison with the coherence model Hao *et al*. (1989) for different shape ratios and two predominant frequencies, 1 and 4 Hz, was conducted and is illustrated in Figs. 9 and 10.

Good agreement between the results of the proposed and Sobczyk′s models were obtained for low shape ratios in which the behavior of the canyon is near to the flat surface.

Figure 12 shows the coherence function between the actual records (measurements) on the Pacoima Dam site (Fig. 11) at Channels 14 and 17 with respect to records of Channel 11 at the base of the canyon during the 2001 earthquake (Taghavi Ghalesari *et al*., 2019; Isari *et al*., 2019). It can be seen that different coherence functions have been achieved for a certain channel under two different earthquakes. Therefore, it can be concluded

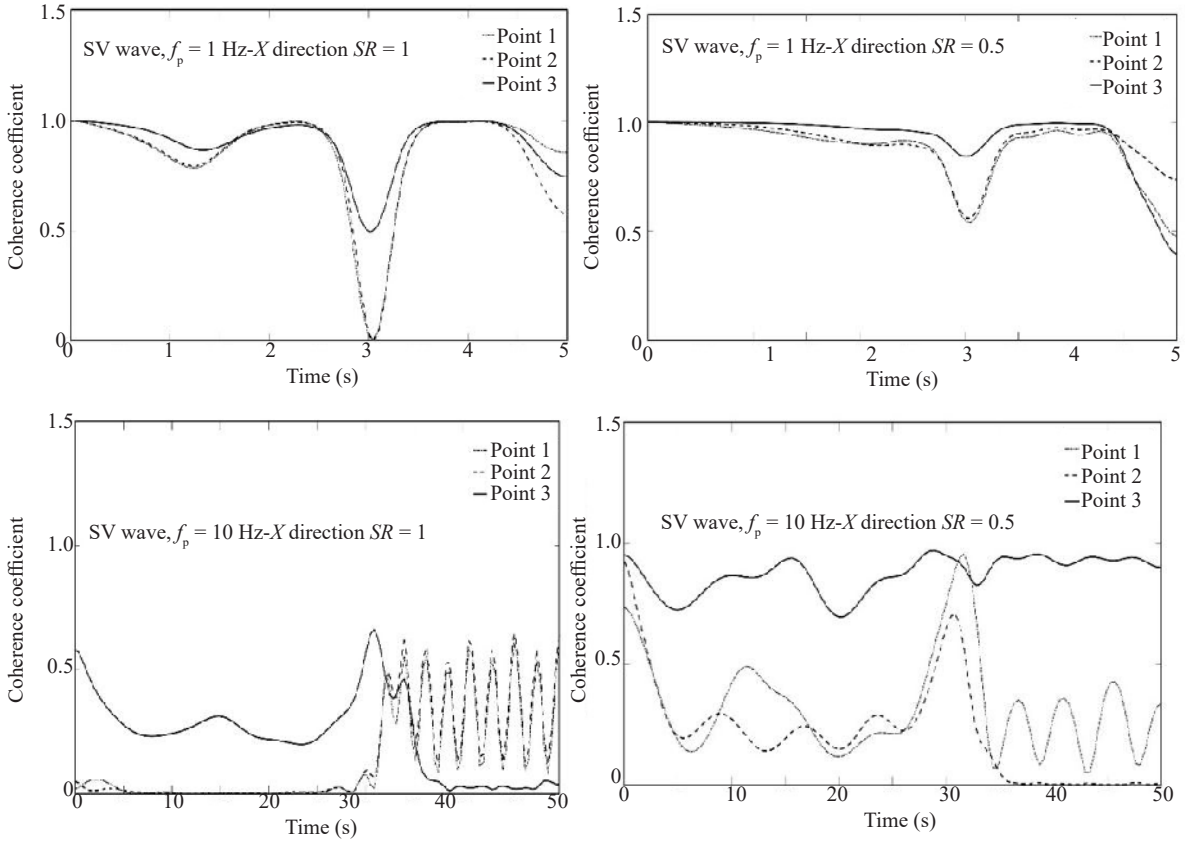

Fig. 7 Comparison of coherence function for different points subjected to the SV wave in the *X*-direction for predominant frequencies of 1 and 10 Hz and SR = 0.5, 1.0

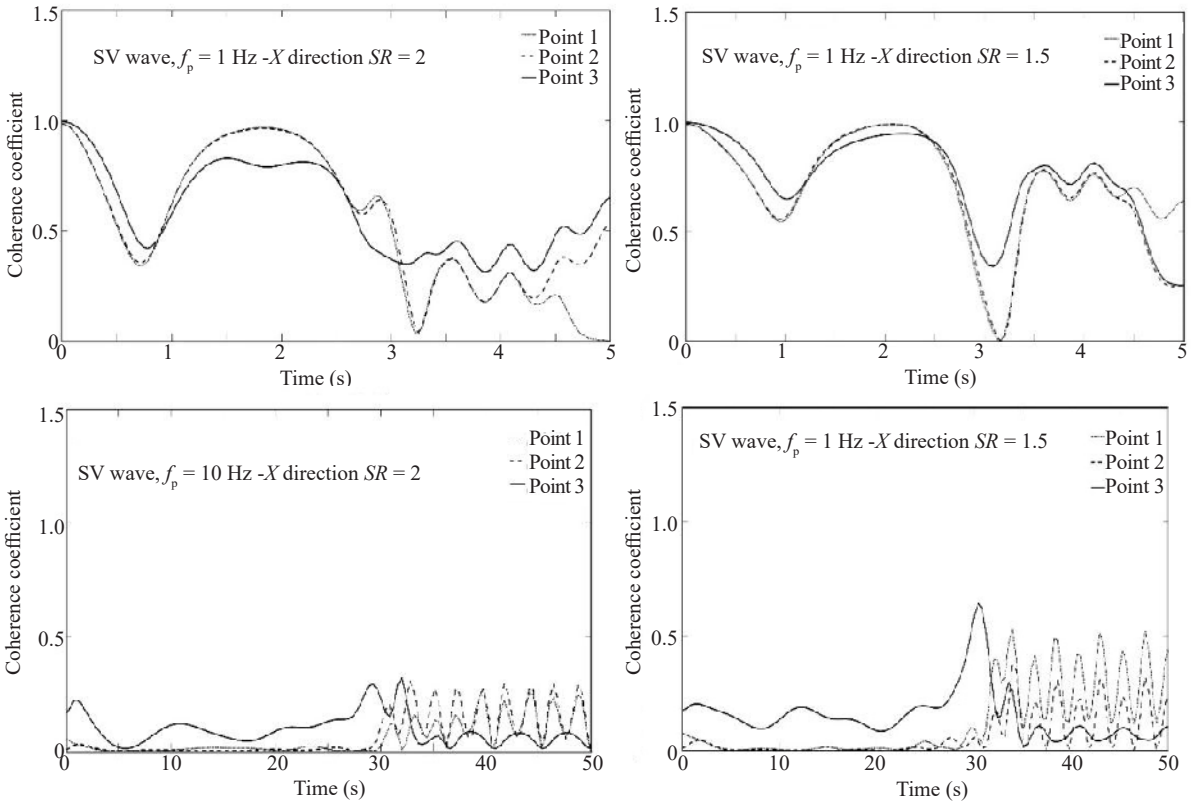

Fig. 8 Comparison of coherence function for different points subjected to the SV wave in the *X*-direction for predominant frequencies of 1 and 10 Hz and *SR* = 1.5, 2

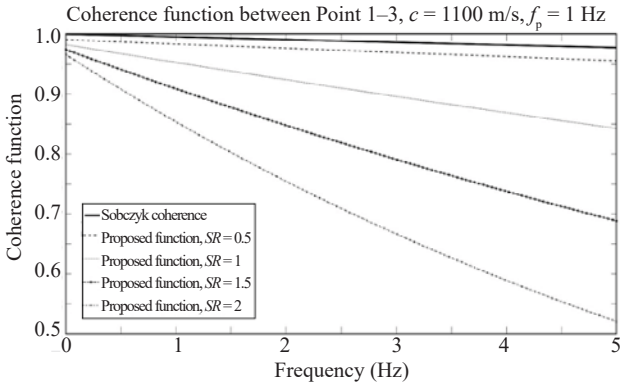

Fig. 9 Comparison of the proposed and Sobczyk′s coherence function for predominant frequency of 1

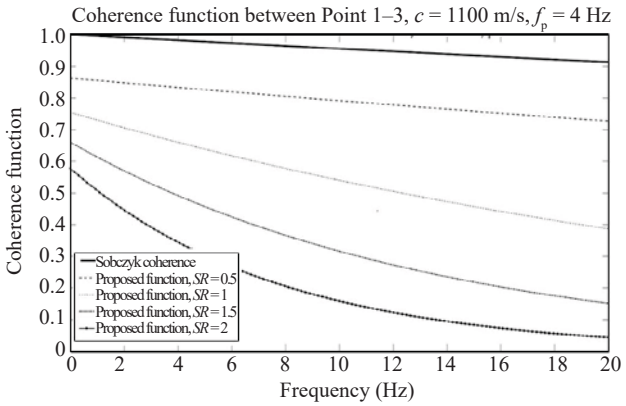

Fig. 10 Comparison of the proposed and Sobczyk′s coherence function for predominant frequency of 4

that the coherence function is also dependent on the characteristics of the incident wave. In addition, during a particular earthquake, different coherence functions were observed for two channels 14 and 17 that have similar elevations from the canyon floor, which means that in addition to the characteristics of the incident wave, the geometric properties of the considered point also influence the coherence function. Moreover, it can be seen that by increasing the frequency, more fluctuations and peaks will appear in the coherence functions of two records. The fluctuated graphs plotted in Fig. 12 were obtained from an earthquake on a real topography (Pacoima dam site), which deals with several influencing factors and complexities (e.g., geometry, material properties). They are not expected to exactly match the curves obtained from numerical modeling. Nevertheless, taking into consideration the initial value and overall trend of the variation of coherence function for different frequencies (which are important parameters), the results indicate good agreement.

3.4 V-shape canyon time-delay function

One of the main parameters of non-uniform ground motion is the time delay between the arrival waves of different points. The waves propagating from a source, for various reasons such as wave passage, soil type and topographic geometry, which results in the refraction and reflection of waves, experience different arrival time

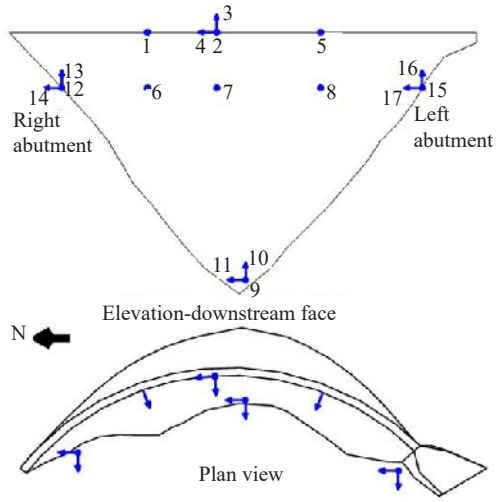

Fig. 11 Arrangement of accelerometers on the Pacoima dam site

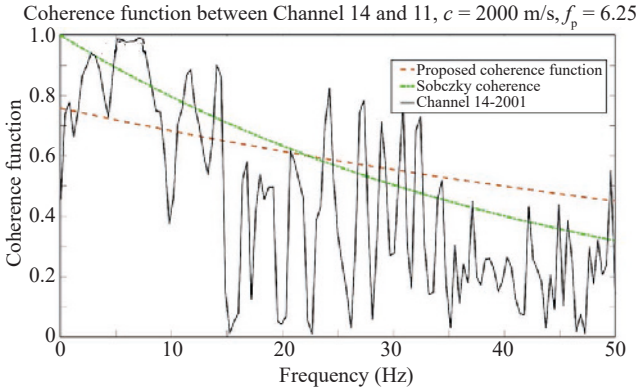

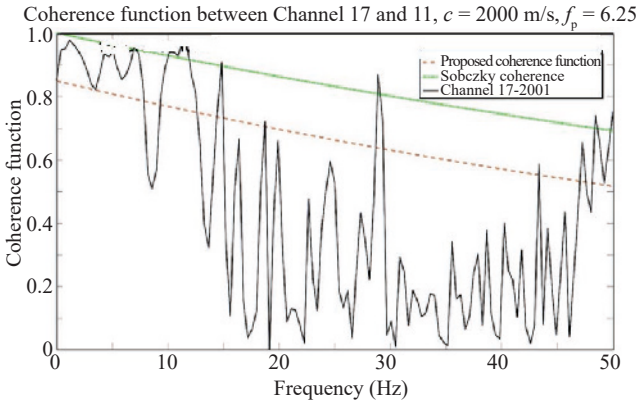

Fig. 12 Coherence functions of Channels 17 and 14 relative to the base channel 11 for f_p = 6.25 Hz obtained from the real records, Sobczyk and the proposed function

at various points. In this study, to evaluate the time delay function, a comprehensive analysis was conducted on V-shape topography at various shape ratios of 0.5 to 2 and subjected to various parameters such as predominant frequency from of 1 to 10 Hz and wave velocity (range of 1000–2000 m/s) and point location (see Table 1). To determine the delay between two signals, the value of time lag resulting from cross-correlation of the signals should be obtained. The cross-correlation between the acceleration of an arbitrary point of the canyon ($a_n(t)$) and the acceleration of the base point of V-shape surface ($a_m(t)$) can be written as (Alves, 2005):

$$-d \le \tau \le d \quad c_{n,m}(\tau) = \int_0^d a_n(t+\tau) a_m(t) \mathrm{d}t$$
$$\tau_{n,m} = \left\{ \tau : c_{n,m}(\tau) \to \max \right\} \tag{8}$$

$c_{n,m}(\tau)$ is cross-correlation between two records. The estimated time delays from the cross correlation are presented in Table 3. The following time delay function was obtained based on the comprehensive parametric analysis for different cases and by using the different regressive functions, which indicated the best agreement with the results of the cross correlation function:

$$\tau_{n,m} = 0.00461 + 2.184 \times (h_{n,m} / c) \times SR - 0.0196 \times (1/f_p) - 1.17259 \times (h_{n,m} / c) \times SR^2 \tag{9}$$

$\tau_{n,m}$ is the time-delay function between two signals (point n) and (point m), $h_{n,m}$ is the height from the base of the canyon, C is the shear wave velocity, SR is the shape ratio and f_p is the predominant frequency. Figure 13 illustrates the time delay curve for different points and different frequencies subjected to the incident SV wave in the X-direction. It is indicated that the time delays for the cases corresponding to the frequencies higher than 5 Hz are constant and independent from the frequency. To verify the proposed time delay function, a comparison between the time delays computed from the January 13, 2001 and 2008 earthquakes acceleration records on the Pacoima Dam (Alves, 2005) and those estimated from the proposed function was performed. The results (see Tables 4 and 5) indicate that the proposed function has good accuracy.

Table 1 Coordinate of considered support points

	SR = 0.5	SR = 1	SR = 1.5	SR = 2
Point A	(200, 0)	(200, 0)	(200, 0)	(200, 0)
Point B	(120, -40)	(120, -80)	(120, -120)	(120, -160)
Point C	(40, -80)	(40, -160)	(40, -240)	(40, -320)
Point D	(0, -100)	(0, -200)	(0, -300)	(0, -400)

Table 2 Coordinate of considered points on the canyon

	SR = 0.5	*SR* = 1	*SR* = 1.5	*SR* = 2
Point *O*	(300, 0)	(300, 0)	(300, 0)	(300, 0)
Point 1	(200, 0)	(200, 0)	(200, 0)	(200, 0)
Point 2	(100, -50)	(100, -100)	(100, -150)	(100, -200)
Point 3	(0, -100)	(0, -200)	(0, -300)	(0, -400)

Table 3 Time delays computed from the base to the support points for incident SV wave (C_s=1100 m/s, *SR*=1.5)

ΔH	f_p=1	f_p=2	f_p=3	f_p=4	f_p=5.5	f_p=6.5	f_p=7.5	f_p=10
0	0	0	0	0	0	0	0	0
61	0.075	0.05	0.05	0.025	0.03	0.03	0.03	0.03
91	0.12	0.075	0.065	0.05	0.045	0.045	0.06	0.06
120	0.14	0.075	0.07	0.05	0.06	0.075	0.075	0.075
157	0.15	0.09	0.075	0.075	0.09	0.09	0.09	0.09
175	0.15	0.1	0.1	0.1	0.105	0.105	0.12	0.12
223	0.17	0.125	0.125	0.125	0.135	0.135	0.135	0.135
266	0.175	0.175	0.15	0.15	0.15	0.165	0.165	0.165
286	0.2	0.175	0.175	0.175	0.165	0.18	0.18	0.18
332	0.225	0.225	0.2	0.2	0.195	0.195	0.195	0.21

Table 4 Comparison of time delays computed from the January 13, 2001 earthquake records and estimated from the proposed function

	N-S (cross-stream)	Estimated
Base to right abutment	$\tau_{17,11}$ = 0.066	0.0638
Base to left abutment	$\tau_{14,11}$ = 0.048	0.041

Table 5 Comparison of time delays obtained from the 2008 earthquake records and estimated from the proposed function

	N-S (cross-stream)	Estimated
Base to right abutment	$\tau_{17,11}$ = 0.02	0.023
Base to left abutment	$\tau_{14,11}$ = 0.03	0.027

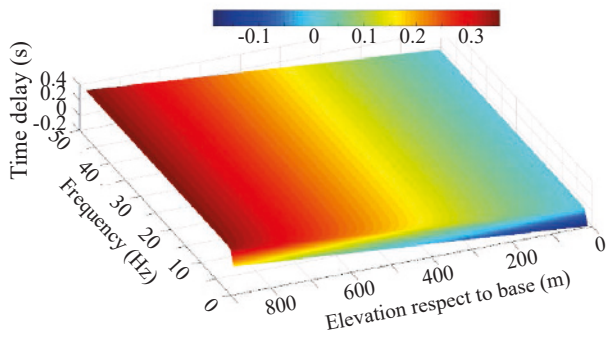

Fig. 13 Estimated time-delay using the proposed function

4 Conclusions

In this paper, a time-domain boundary element method was used for comprehensive parametric analysis on the dynamic behavior of V-shape canyons subjected to the SV wave. The main conclusions of this study are summarized as follows:

1. One of the main parameters in the simulation of non-uniform ground motion is coherence function. Increasing shape ratio and predominant frequency on a canyon surface is shown to decrease the coherence between two time-domain responses.

2. Based on the effective parameters, a new coherence function was developed for generation of non-uniform ground motion on topographic site. Its accuracy was indicated in a comparison against the results of Sobczyk′s coherence model.

3. Time-delay between the arrival of waves to points on the canyon surface is one of the main parameters used for generation of non-uniform records. Results indicated that time delay is dependent on shape ratio, wave velocity, predominant frequency and elevation from the base of the canyon.

4. A time delay function considering the effective parameters was proposed. Its efficiency and accuracy was indicated by 21 January 2001 and 2008 earthquake records on the Pacoima dam site in comparison with the former literature results.

Acknowledgement

The authors would like to express their gratitude

to Dr. Mohsen Kamalian (International Institute of Earthquake Engineering and Seismology) and Abbasali Taghavi Ghalesari (University of Texas at El Paso) for their suggestions and comments.

References

Abrahamson NA (1993), "Spatial Variation of Multiple Support Inputs," *Proceedings of the 1st US Seminar on Seismic Evaluation and Retrofit of Steel Bridges*, San Francisco, CA.

Alves SW (2005), "Nonlinear Analysis of Pacoima Dam with Spatially Non-Uniform Ground Motion," *PhD Dissertation*, California Institute of Technology, Pasadena, California.

Der Kiureghian A and Neuenhofer A (1992), "Response Spectrum Method for Multiple- Support Seismic Excitation," *Earthquake Engineering and Structural Dynamics*, **21**: 712–40.

Gatmiri B, Maghoul P and Arson C (2008), "Site-Specific Spectral Response of Seismic Movement due to Geometrical and Geotechnical Characteristics of Sites," *Soil Dynamics and Earthquake Engineering*, doi: 10.1016/j.soildyn.01.015.

Gao YF (2019), "Analytical Models and Amplification Effects of Seismic Wave Propagation in Canyon Sites," *Chinese Journal of Geotechnical Engineering*, **41**(1): 1–25.

Hao H, Oliveira CS and Penzien J (1989), "Multiple-Station Ground Motion Processing and Simulation Based on SMART-1 Array Data," *Nuclear Engineering and Design*, **111**(3): 293–310.

Harichandran RS and Vanmarcke EH (1986), "Stochastic Variation of Earthquake Ground Motion in Space and Time," *Journal of the Engineering Mechanics Division*, **112**: 154–74.

Hesami S, Ahmadi S and Taghavi Ghalesari A (2015), "Numerical Modeling of Train-Induced Vibration of Nearby Multi-Story Building: a Case Study," *KSCE Journal of Civil Engineering*, **20**(5): 1701–1713.

Huang HC and Chiu HC (1995), "The Effect of Canyon Topography on Strong Ground Motion at Feitsui Damsite: Quantitive Results," *Earthquake Engineering and Structural Dynamics*, **24**(7): 977–990.

Isari M, Tarinejad R, TaghaviGhalesari A and Sohrabi-Bidar A (2019), "A New Approach to Generating Non-Uniform Support Excitation at Topographic Sites," *Soils and Foundations*, **59**(6): 1933–1945.

Kamalian M, Gatmiri B, Sohrabi-Bidar A and Khalaj A (2007), "Amplification Pattern of 2D Semi-Sine-Shaped Valleys Subjected to Vertically Propagating Incident Waves," *Communications in Numerical Methods in Engineering*, **23**: 871–887.

Kamalian M, Gatmiri B and Sohrabi-Bidar A (2003), "On Time-Domain Two-Dimensional Site Response Analysis of Topographic Structures by BEM," *Journal of Seismology and Earthquake Engineering*, **5**(2): 35–45.

Kamalian M, Jafari MK, Sohrabi-Bidar A, Razmkhah A and Gatmiri B (2006), "Time-Domain Two-Dimensional Site Response Analysis of Non-Homogeneous Topographic Structures by a Hybrid FE / BE Method," *Soil Dynamics and Earthquake Engineering*, **26**: 753–765.

Luco JE and Wong HL (1986), "Response of a Rigid Foundation to a Spatially Random Ground Motion," *Earthquake Engineering and Structural Dynamics*, **14**: 891–908.

Mossessian TK and Dravinski M (1990a), "Amplification of Elastic Waves by a Three Dimensional Valley. Part1: Steady-State Response," *Earthquake Engineering and Structural Dynamics*, **19**(5): 667–680.

Mossessian TK and Dravinski M (1990b), "Amplification of Elastic Waves by a Three Dimensional Valley. Part2: Transient Response," *Earthquake Engineering and Structural Dynamics*, **19**(5): 681–691.

Paolucci R (2002), "Amplification of Earthquake Ground Motion by Steep Topographic Irregularities," *Earthquake Engineering and Structural Dynamics*, **31**(10): 1831–1853.

Sohrabi-Bidar A, Kamalian M and Jafari MK (2009), "Time-Domain BEM for Three-Dimensional Site Response Analysis of Topographic Structures," *International Journal for Numerical Methods in Engineering*, **79**: 1467–1492.

Sohrabi-Bidar A, Kamalian, M and Jafari MK (2010), "Seismic Response of 3D Gaussian Shaped Valleys to Vertically Propagating Incident Waves," *Geophysical Journal International*, **183**: 1429–1442.

Sohrabi-Bidar and Kamalian M (2013), "Effects of Three-Dimensionality on Seismic Response of Gaussian-Shaped Hills for Simple Incident Pulses," *Soil Dynamics And Earthquake Engineering*, **52**: 1–12.

Taghavi Ghalesari A, Isari M, Tarinejad R and Sohrabi-Bidar A (2019), "A Procedure to Predict the Precise Seismic Response of Arch Dams in Time Domain Using Boundary Element Formulation," *Journal of Rock Mechanics and Geotechnical Engineering*, **11**(4): 790–803.

Tarinejad R, Fatehi R and Harichandran RS (2013), "Response of an Arch Dam to Non-Uniform Excitation Generated by a Seismic Wave Scattering Model," *Soil Dynamics and Earthquake Engineering*, **52**: 40–54.

Tarinejad R, Isari M and Sohrabi-Bidar A (2020), "A New Solution to Estimate the Time Delay on the Topographic Site Using Time Domain 3D Boundary Element Method," *Earthquake Engineering and Engineering Vibration*, **19**(3): 611–623. https://doi.org/10.1007/s11803-020-0584-8.

Tarinejad R, Isari M and Taghavi Ghalesari A (2019), "A New Boundary Element Solution to Evaluate the Geometric Effects of the Canyon Site on the Displacement Response Spectrum," *Earthquake Engineering and Engineering Vibration*, **18**(2): 267–284. https://doi.org/10.1007/s11803-019-0503-z

Tsaur DH and Chang KH (2008), "An Analytical Approach for the Scattering of SH Waves by a Symmetrical V-Shaped Canyon: Shallow Case," *Geophysical Journal International*, **174**(1): 255–264.

Zhang L and Chopra AK (1991), "Three-Dimensional Analysis of Spatially Varying Ground Motions Around a Uniform Canyon in a Homogeneous Half-Space," *Earthquake Engineering and Structural Dynamics*, **20**: 911–926.

Zhao C and Valliappan S (1993), "Incident P and SV Wave Scattering Effects Under Different Canyon Topographic and Geological Conditions," *Int. J. Num. Analy. Methods in Geomechanics*, **17**(2): 73–94.